Chandra ACIS Survey of M33 (ChASeM33): The X-ray Point Source Population of M33

M. Sasaki (CfA), B. Williams (University of Washington), P. Plucinsky (CfA), W. Pietsch (MPE), T. J. Gaetz (CfA), K. S. Long (STScI), T. Mazeh (Tel Aviv University), A. Shporer (Tel Aviv University), F. Haberl (MPE), T. G. Pannuti (Morehead State University), P. Ghavamian (JHU), L. Bianchi (JHU), A. Tolea (JHU), and the ChASeM33 team

With most of the 1.4 Ms of Chandra ACIS M33 data already available, we have begun measuring the properties of the hundreds of sources present in the data. To date nearly 600 discrete sources have been cataloged, over 90% of these objects are point sources closely matching the Chandra point spread function. The high spatial resolution (about 1 arcsecond) has made separating point and extended sources more straightforward over a larger region of M33 than ever before. Spectral and timing analyses of the current source catalog have provided hardness ratios and variability information to aid in initial source classification. The full catalog of X-ray binaries will provide an X-ray Luminosity Function (XLF) down to luminosities of around 1e35 erg/s (at the 3-sigma level). Such an XLF will allow detailed studies of the interplay between star formation and X-ray source formation, providing a new level of detail in the understanding of galaxy evolution from one end of the stellar life cycle to the other. Finally, the data set is a treasure trove of exotic X-ray sources, such as new transient X-ray sources, the first eclipsing black hole binary, and a new eclipsing high mass X-ray binary.

This work was supported by NASA Chandra award number G06-7073A.

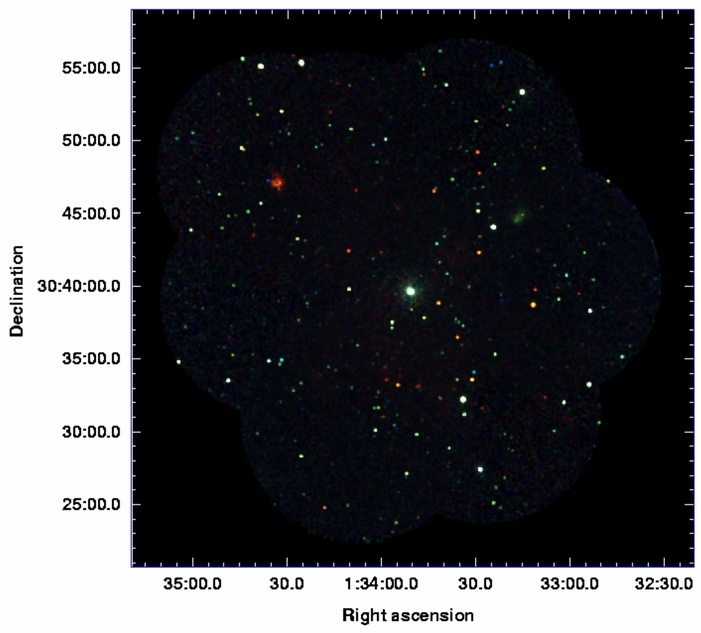

Fig. 1 Exposure corrected mosaic image of ChASeM33 observations of M33 (red: 0.35-1.1 keV, green: 1.1-2.6 keV, blue:2.6-8.0 keV). Previous ACIS-I observations (ObsIDs 1730 and 2023) are included as well. Events within 8arcmin off-axis angle are used.

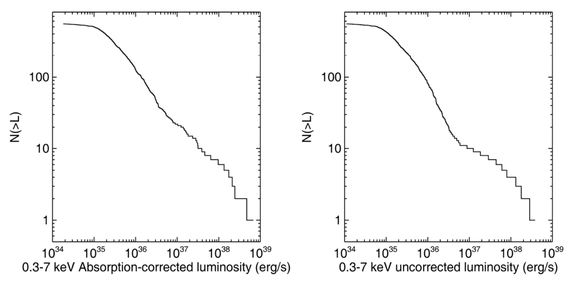

Fig. 3 Log(N) - log(L) diagrams of the point sources detected in the ACIS-I data of ChASeM33.

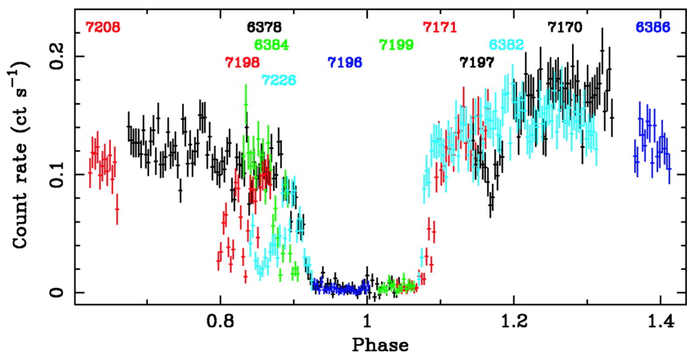

Fig. 4 Chandra ACIS light curve of the X-ray binary X-7 in the 0.5–5.0 keV band. Individual observations are marked by their ObsID.

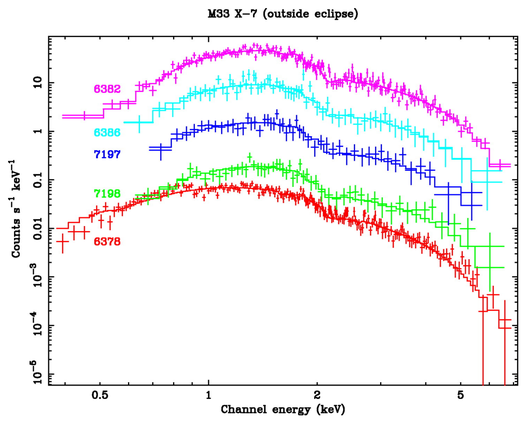

Fig. 6 Chandra ACIS spectra of X-7 during high state. Data and the corresponding disk blackbody model (with inner disk temperature kT = 0.99 ± 0.03 keV and N_H = (0.95 ± 0.10) × 10^{21} cm^{-2}) are shown. For a better representation, the spectra were multiplied successively by factors of 1, 5, 5^2, 5^3, and 5^4 from the bottom to the top.

ChASeM33 Point Source Catalog

We ran the CIAO tool *wavdetect* on data of each field in the bands S=0.35-1.1 keV, M=1.1-2.6keV, H=2.6-8.0 keV, and B=0.35-8.0 keV to perform source detection. From the output source lists of *wavdetect* we selected sources with source significance > 3 sigma to create the final source list. We measured all of the fluxes, spectra, and timing for our final source list using the software package ACIS Extract. This software allows a visual inspection of each source in each exposure along with an outline of the point spread function in that location of the ACIS field of view. These visual inspections allowed us to flag extended sources in the catalog and remove duplicate sources that were observed in overlapping sections of fields.

So far, we have identified SNRs and candidates by cross-correlation with the catalog of optical SNRs (Gordon et al., 1998, ApJS, 117, 89; GKL98). The hardness ratio diagram in Figure 2 shows that the SNRs are mainly located in a region with HR1 < 0, -0.5 < HR2 < 0, whereas most of the point sources have HR1 ≈ 0, HR2 ≈ 0.

We converted the fluxes to luminosities assuming the incident photon spectrum is an absorbed power-law with Γ = 1.9 and NH = 1e21 cm^{-2} at a distance of 820 kpc. These luminosities were used to plot the log(N)-log(L) diagrams in Figure 3.

First Eclipsing Black Hole Binary

The ChASeM33 observations sampled the eclipsing X-ray binary M33 X-7 over a large part of the 3.45 day orbital period and have resolved eclipse ingress and egress for the first time (Fig. 4). The occurrence of the X-ray eclipse allows us to determine an improved ephemeris of mid-eclipse and binary period as HJD (2,453,639.119+/-0.005)+/-N(3.453014+/-0.000020) (Fig. 5) and constrain the eclipse half-angle to 26.5d+/-1.1d. There are indications for a shortening of the orbital period. The X-ray spectrum is best described by a disk blackbody spectrum typical for black hole X-ray binaries in the Galaxy (Fig. 6). We find a flat power density spectrum, and no significant regular pulsations were found in the frequency range of 1e-4 to 0.15 Hz. HST WFPC2 images resolve the optical counterpart, which can be identified as an O6 III. Based on the optical light curve, the mass of the compact object in the system most likely exceeds 9 Msolar. This mass, the shape of the X-ray spectrum, and the short-term X-ray time variability identify M33 X-7 as the first eclipsing black hole high-mass X-ray binary.

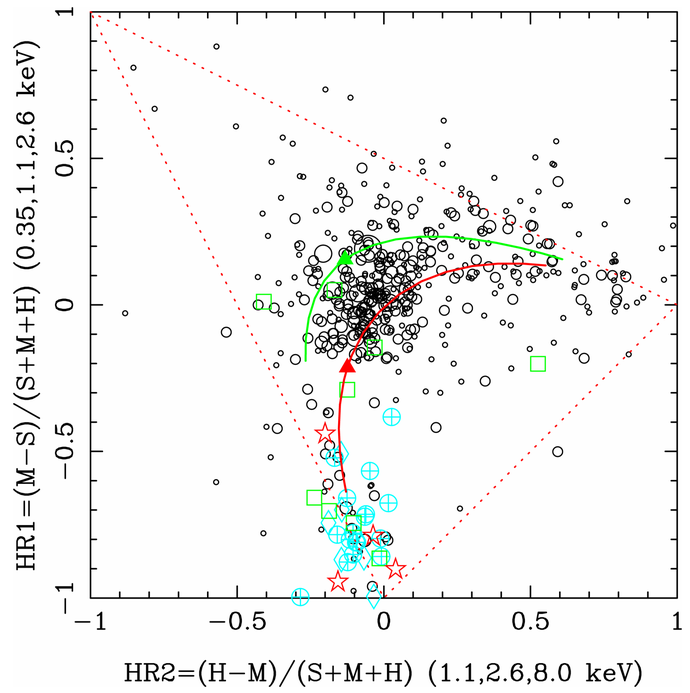

Fig. 2 Hardness ratio plot constructed from the ChASeM33 source catalog. Unidentified sources are plotted as black circles with symbol size indicating the flux: photon flux < 1e-6 phot/s/cm^2 (smallest), 1e-6 < photon flux <= 1e-5 phot/s/cm^2, etc., 1e-3 phot/s/cm^2 < photon flux (largest). In addition, the sources identified as SNRs through cross-correlation with the optical SNR catalog by GKL98, other extended sources, and soft band sources are encoded as colored symbols: GKL98 nonextended (cyan diamond), GKL98 extended (cyan earth), other extended (green square), soft band (red star). The solid red curve (solid green curve) indicate the locus of power-laws with Γ = 0 to 3 with different NH. The red curve assumes NH = 1e21 cm^{-2}, while the green curve assumes NH = 3e21 cm^{-2}. The solid red (green) triangles indicate the Γ = 1.9 power-law.

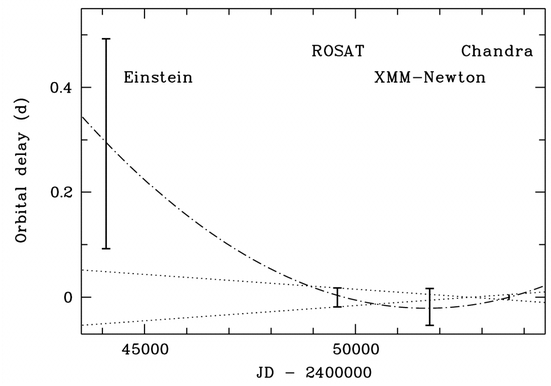

Fig. 5 Deviation of eclipse egress times relative to the best orbital period of 3.453014 days and Chandra eclipse egress ephemeris for M33 X-7. The dotted lines give the shortest and longest periods allowed by the Chandra and ROSAT data. The parabola assumes a period of 3.45294 days at the Chandra epoch, and orbital period decay rate of P_dot_{orb}/P_{orb} = -4 × 10^{-6} yr^{-1} .

Second Eclipsing X-ray Binary

The variable XMM-Newton source [PMH2004] 47 was identified as an XRB candidate by Misanovic et al. (2006, A&A 448, 1247), varying strongly in brightness during the XMM-Newton observations from 2000 to 2003. During the ChASeM33 observations on 2006 September 18/19 the source was bright and there was a drop to an intensity consistent with zero for about 25 ks. We interpret this as an eclipse of the X-ray source. Ingress and egress transitions take no longer than 500 s each. During the bright phase the source shows a hard X-ray spectrum with an absorption column density of 2.2x10^21 cm^-2 and a photon index of 0.97 when modeled with an absorbed power-law. On 2006 September 26 the source showed another transition from low to intermediate intensity. We derive an orbital period of 1.73245 d, a mid-eclipse epoch of JD2453997.470, and an eclipse half angle of 30.7 degrees. The position of the source coincides with star #4571 of Massey et al. (2006, AJ 131, 2478) which shows V=21.011 mag and colors consistent with a B0V to B2III star after extinction and color correction.

This star was not identified as variable in the M33 CFHT variability survey (Hartman et al. 2006, MNRAS, 371, 1405). To search for any small optical modulation, we derive the light curves of this star in the Sloan *g'*, *r'* & *i'* bands directly from the CFHT images. Folding the 31-33 measurements in each of these colors with the X-ray period reveals a clear periodicity. The folded light curve is of double sinusoidal shape, with one of the minima at the phase of mid X-ray eclipse, suggesting an ellipsoidal modulation of a high-mass optical companion. [PMH2004] 47 is therefore most likely the second eclipsing HMXB in M33 after the eclipsing black hole X-ray binary M33 X-7.